for the thermogravimetric analyses. A portion of this work was performed under NASA Grant NSG-1124 with Virginia Polytechnic Institute and State University, Blacksburg, VA 24061.

References and Notes

(1) Hergenrother, P. M. *Polym. Eng. Sci.* **1976**, *16* (5), 303.
(2) Hergenrother, P. M.; Levine, H. H. *J. Polym. Sci., Part A-1* **1967**, *5*, 1453.
(3) Hergenrother, P. M. *Macromolecules* **1974**, *7*, 575.
(4) Rafter, R. T.; Harrison, E. S. *Am. Chem. Soc., Div. Org. Coat. Plast. Chem., Prepr.* **1975**, *35* (2), 204.
(5) Hedberg, F. L.; Arnold, F. E. *J. Polym. Sci., Polym. Chem. Ed.* **1974**, *12*, 1925.
(6) Wentworth, S. E.; Mulligan, G. D. *Am. Chem. Soc., Div. Polym. Chem., Prepr.* **1974**, *15* (1), 697.
(7) Hedberg, F. L.; Arnold, F. E. *J. Polym. Sci., Polym. Chem. Ed.* **1976**, *14*, 2607.
(8) Arnold, F. E. U.S. Patent Application 678,324 (to U.S. Department of the Air Force); *Chem. Abstr.* **1977**, *86*, 7379a.
(9) Banihashemi, A.; Marvel, C. S. *J. Polym. Sci., Polym. Chem. Ed.* **1977**, *15*, 2653.
(10) Harris, F. W.; Padaki, S. M.; Varaprath, S. *Am. Chem. Soc., Div. Polym. Chem., Prepr.* **1980**, *21* (1), 3 (abstract only).
(11) Hergenrother, P. M. *Macromolecules* **1981**, *14*, 891.
(12) Hergenrother, P. M. *J. Polym. Sci., Part A-1* **1969**, *7*, 949.
(13) Ogliaruso, M. A.; Shadoff, L. A.; Becker, E. I. *J. Org. Chem* **1963**, *28*, 2725.
(14) Hergenrother, P. M. *J. Macromol. Sci., Chem.* **1971**, *A5* (2), 365.
(15) Wrasidlo, W.; Augl, J. M. *J. Polym. Sci., Part A-1* **1969**, *7*, 3393.
(16) Hergenrother, P. M. *J. Appl. Polym. Sci.* **1974**, *18*, 1779.
(17) Vogel, H.; Marvel, C. S. *J. Polym. Sci.* **1961**, *50*, 511.
(18) Hergenrother, P. M.; Sykes, G. F.; Young, P. R. *Am. Chem. Soc., Div. Pet. Chem., Prepr.* **1979**, *24* (1), 243.
(19) Hergenrother, P. M. *Polym. Eng. Sci.* **1976**, *16* (5), 303.

Rodlike Nature of α-Helical Polypeptides in Solution

Satoru Itou,[1] Noboru Nishioka,[2] Takashi Norisuye, and Akio Teramoto*

Department of Macromolecular Science, Osaka University, Toyonaka, Osaka 560, Japan.
Received April 18, 1980

ABSTRACT: Light scattering, viscosity, and sedimentation measurements were performed on solutions of poly(ϵ-carbobenzoxy-L-lysyl-γ-benzyl-L-glutamate) in *N,N*-dimethylformamide to obtain the light scattering radius $\langle S^2\rangle_z^{1/2}$, intrinsic viscosity $[\eta]$, and limiting sedimentation coefficient s_0 as functions of molecular weight. The results showed that the α helix of this polypeptide is intact and straight at weight-average molecular weights lower than 200 000 but exhibits flexibility at higher molecular weights. The data for $[\eta]$ and s_0 in the lower molecular weight region combined with similar data for poly(γ-benzyl L-glutamate) in *N,N*-dimethylformamide were analyzed by the hydrodynamic theories of Norisuye et al. and Yoshizaki and Yamakawa for cylindrical molecules, yielding molecular dimensions consistent with the α helices of these polypeptides.

Doty et al.[3] were the first to show from light scattering and viscosity data that poly(γ-benzyl L-glutamate) (PBLG) is α-helical in *N,N*-dimethylformamide (DMF) and $CHCl_3$ and behaves as a rigid rod. Subsequent studies on various synthetic polypeptides,[4-7] however, have revealed that the polypeptide chain in the α-helical conformation exhibits flexibility as it becomes very long. It has also been shown[7,8] that although low molecular weight PBLG and poly(ϵ-carbobenzoxy-L-lysine) (PCBL) are rodlike in DMF at room temperature, PCBL is more flexible than PBLG at high molecular weight. This is ascribed to the difference in helix stability between these polypeptides in helix-supporting solvents.[9,10] Since the helix stability is related to the chemical structure of the polypeptide chain, it is interesting to study sequential polypeptides consisting of γ-benzyl-L-glutamyl and ϵ-carbobenzoxy-L-lysyl residues. In a previous publication[11] we have shown that poly(ϵ-carbobenzoxy-L-lysyl-γ-benzyl-L-glutamate) (poly[Lys(Cbz)-Glu(OBzl)]) assumes an α-helical conformation in DMF, 2,2,2-trifluoroethanol, and other helix-supporting solvents. In this study we made light scattering, viscosity, and sedimentation measurements on dilute solutions of poly[Lys(Cbz)-Glu(OBzl)] in DMF. The light scattering data obtained are compared with similar data for PBLG and PCBL to examine whether or not a poly[Lys(Cbz)-Glu(OBzl)] molecule takes the shape of a rigid rod. The viscosity and sedimentation data for poly[Lys(Cbz)-Glu(OBzl)] together with those for PBLG are analyzed by recent hydrodynamic theories for cylindrical molecules.[12,13]

Experimental Methods

Polypeptide Samples. The poly[Lys(Cbz)-Glu(OBzl)] samples LG-1 through LG-10 were used: LG-1 and LG-4 were those used previously[14] (CF-H-2 and CF-F-2, respectively, in the previous designation) and the rest were the fractions chosen from our stock.[11,14] The PBLG samples used for viscosity measurements were those characterized in our previous study[15] (Table I).

Table I
Viscosity Data for Poly(γ-benzyl L-glutamate)[a]

sample code	$\bar{M}_w \times 10^{-4}$	$\bar{M}_n \times 10^{-4}$	$[\eta] \times 10^{-2}$/cm^3 g^{-1} DMF, 25 °C	$[\eta] \times 10^{-2}$/cm^3 g^{-1} DCA,[b] 25 °C
A-1	0.347		0.0378	0.0715
A-2	0.476		0.0374	0.083
A-3	1.06		0.055	0.121
A-4	1.42		0.0745	0.152
A-5	2.21		0.120	0.205
A-6	3.70	3.20	0.238	0.301
A-IV	6.35	5.49	0.526	0.450
E-4	8.08	7.14	0.708	0.547
E-3	15.8	12.8	1.94	0.898
A-X	18.8		2.42	0.98
E-2	23.7		3.62	1.22
A-IX	35.4		6.0	1.60
F-2	47.7		9.20	2.17
E-1	56.7	42.2	12.8	2.48

[a] The data for A-IV through E-1 have been taken from ref 23. [b] DCA = dichloroacetic acid.

Light Scattering. Intensities of light scattered from solutions of poly[Lys(Cbz)-Glu(OBzl)] in DMF at 25 °C were measured by using a FICA 50 photogoniometer[16] with vertically polarized incident light of wavelengths of 436 and 546 nm at scattering angles ranging from 15 to 150°. The photogoniometer was calibrated with benzene at 25 °C as the standard liquid by taking the Rayleigh ratio to be 46.5×10^{-6} cm^{-1} at 436 nm and 16.1×10^{-6} cm^{-1} at 546 nm.[17] The data were extrapolated to infinite dilution and zero scattering angle by Berry's method.[18] Polymer

0024-9297/81/2214-0904$01.25/0

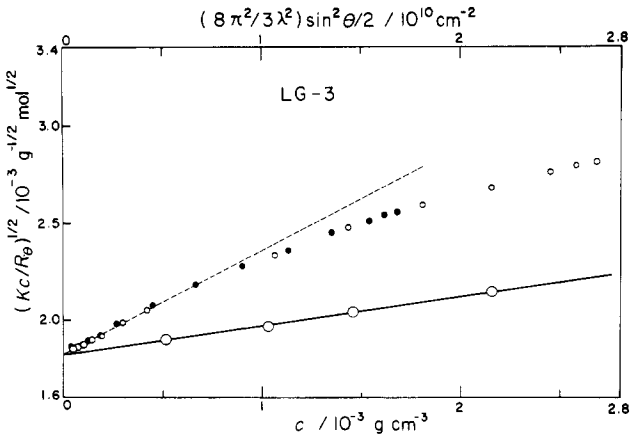

Figure 1. Concentration dependence of $(Kc/R_\theta)^{1/2}$ at zero scattering angle (lower abscissa) and angular dependence of $(Kc/R_\theta)^{1/2}$ at infinite dilution (upper abscissa) for poly[Lys-(Cbz)-Glu(OBzl)] sample LG-3 in DMF at 25 °C. The smaller unfilled and filled circles denote the data for 436 and 546 nm, respectively. The dashed line indicates the initial tangent.

solutions and the solvent were made dust-free by centrifugation at 34000*g* for 2–3 h in a Sorvall RC2-B centrifuge, and the central part of the solution in the centrifuge tube was pipetted directly into the scattering cell.

The specific refractive index increment at infinite dilution, $(\partial n/\partial c)_0$, for poly[Lys(Cbz)-Glu(OBzl)] in DMF at 25 °C was 0.121 cm³ g⁻¹ at 436 nm and 0.119 cm³ g⁻¹ at 546 nm, when measured with a differential refractometer of the Schulz-Cantow type. These values are quite close to those reported for PBLG[3,19] and PCBL[8] in the same solvent.

Viscosity. Viscosity measurements were made on solutions of poly[Lys(Cbz)-Glu(OBzl)] in DMF at 25 °C and those of PBLG in DMF and in dichloroacetic acid at 25 °C. No kinetic energy correction was needed. The effect of shear rate on intrinsic viscosity ($[\eta]$) was not appreciable unless $[\eta]$ exceeded 800 cm³ g⁻¹, as checked by a rotational viscometer of the Zimm-Crothers type.[20]

Sedimentation. Sedimentation velocities of poly[Lys-(Cbz)-Glu(OBzl)] in DMF at 25 °C were measured at polymer concentrations ranging from 5×10^{-4} to 9.4×10^{-3} g cm⁻³. A Beckman Spinco Model E ultracentrifuge was used with either a 12-mm aluminum single-sector cell or a 30-mm Kel-F single-sector cell. Rotor speeds were chosen at 52000, 48000, or 44000 rpm, depending on the sample and the initial concentration. The partial specific volume $\bar{v}$ of poly[Lys(Cbz)-Glu(OBzl)] in DMF at 25 °C was assumed to be 0.795 cm³ g⁻¹, which is the average of those for PBLG[19] (0.786 cm³ g⁻¹) and PCBL[8] (0.803 cm³ g⁻¹). The density and viscosity of DMF at 25 °C were found to be 0.9439 g cm⁻³ and 8.0×10^{-3} g cm⁻¹ s⁻¹, respectively.

Experimental Results

Light Scattering. Figure 1 shows typical light scattering results for sample LG-3, where R_θ is the Rayleigh ratio at the scattering angle θ and concentration c (g cm⁻³) and λ is the wavelength of light in the scattering medium. The data points at infinite dilution, $(Kc/R_\theta)_{c=0}^{1/2}$, for 436 and 546 nm plotted against $(8\pi^2/3\lambda^2)\sin^2(\theta/2)$ fall on a single curve, with the initial tangent indicated by a dashed line. The data points for $(Kc/R_0)^{1/2}$ vs. c follow closely a straight line with the ordinate intercept common to the dashed line. These straight lines are used to evaluate the weight-average molecular weight ($\bar{M}_w$), the second virial coefficient (A_2), and the z-average mean-square radius of gyration ($\langle S^2\rangle_z$) of the sample.

Figure 2 shows values of $(Kc/R_0)^{1/2}$ plotted against c for ten poly[Lys(Cbz)-Glu(OBzl)] fractions in DMF at 25 °C. The values of $\bar{M}_w$ and A_2 obtained from these plots are summarized in Table II.

The particle scattering functions $P(\theta)$ of the poly[Lys-(Cbz)-Glu(OBzl)] fractions in DMF at 25 °C are shown in

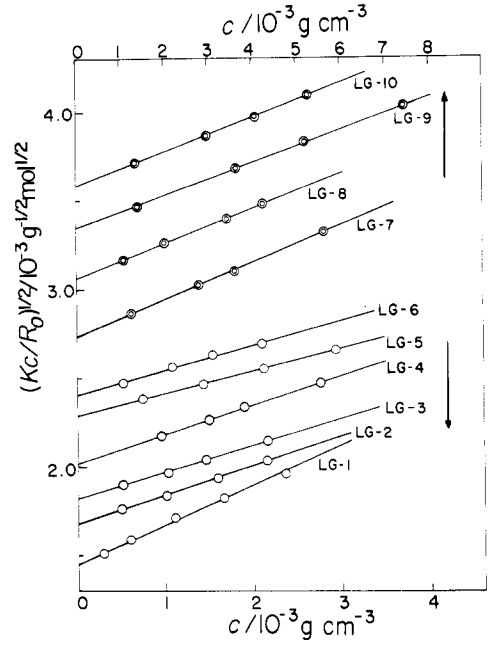

Figure 2. Concentration dependence of $(Kc/R_0)^{1/2}$ for poly-[Lys(Cbz)-Glu(OBzl)] samples in DMF at 25 °C.

Table II
Light Scattering Data for Poly[Lys(Cbz)-Glu(OBzl)] in DMF at 25 °C

sample code	$\bar{M}_w \times 10^{-4}$	$A_2 \times 10^4$/ g⁻² cm³ mol	$\langle s^2\rangle_z^{1/2}$/nm
LG-1[a]	47.6	3.24	75.2
LG-2	35.4	1.93	56.7
LG-3	30.2	2.72	54.1
LG-4[b]	24.6	3.39	43.2
LG-5	19.1	2.86	35.1
LG-6	17.3	3.39	30.7
LG-7	13.4	2.87	26.2
LG-8	10.7	3.04	21.2
LG-9	8.9_4	3.07	17.3
LG-10	7.7_9	3.46	15.6

[a] Designated CF-H-2 in ref 14; $\bar{M}_n = 35.5 \times 10^4$. [b] Designated CF-F-2 in ref 14; $\bar{M}_n = 20.9 \times 10^4$.

Figure 3. For each fraction the data points for 436 and 546 nm fall on a single curve. The initial slope of the curve is larger for higher molecular weight, indicating that $\langle S^2\rangle_z$ is an increasing function of molecular weight. The dotted and dot–dash curves for LG-1 represent $P(\theta)^{-1/2}$ for a monodisperse rod and that for a monodisperse Gaussian coil, respectively, both having $\langle S^2\rangle$ equal to $\langle S^2\rangle_z$ of LG-1. The curve for the Gaussian coil deviates sharply upward from the experimental curve. This implies that the conformation of the polypeptide chain cannot be a random coil. The data points come close to the rod curve. The values of $\langle S^2\rangle_z$ obtained from these plots are given in Table II.

Figure 4 shows the dependence of the root-mean-square radius of gyration on the degree of polymerization for poly[Lys(Cbz)-Glu(OBzl)] in DMF at 25 °C, where the data for PBLG[6] and PCBL[8,21] in the same solvent are compared. Here $\bar{N}_w$ stands for the weight-average number of peptide residues per molecule. The data obtained by Doty et al.[3] and Moha et al.[22] for PBLG exhibit essentially the same molecular weight dependence as that shown here. We have not reproduced them so as to avoid confusion. The straight line in Figure 4 represents the values of $\langle S^2\rangle_z^{1/2}$ for the α-helical polypeptide with the helical pitch per monomeric residue 0.15 nm. For $\bar{N}_w$ smaller than 1000,

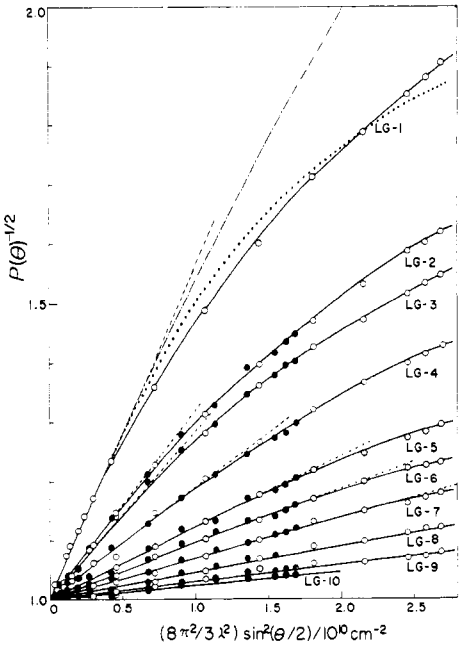

Figure 3. Angular dependence of $P(\theta)^{-1/2}$ for poly[Lys(Cbz)-Glu(OBzl)] samples in DMF at 25 °C. The unfilled and filled circles denote the data for 436 and 546 nm, respectively; the dashed line for each sample represents the initial tangent to the curve, and the dotted and dot–dash lines indicate the $P(\theta)^{-1/2}$ values for a straight rod and a Gaussian coil, respectively (see text).

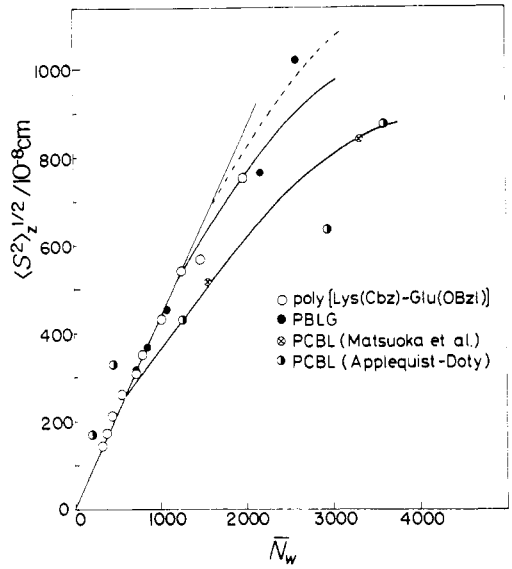

Figure 4. Plots of $\langle S^2\rangle_z^{1/2}$ vs. $\bar{N}_w$ for the three indicated polypeptides in DMF at 25 °C. The straight line represents the values expected for the straight α-helical rods.

all the data points but two PCBL points come close to this line. Thus, we conclude that the helices of these polypeptides are α-helical and intact in this range of $\bar{N}_w$. At larger $\bar{N}_w$, however, the data tend to deviate downward from the straight line. This downward deviation is ascribed to the onset of chain flexibility. When compared at the same $\bar{N}_w$, the values of $\langle S^2\rangle_z$ for poly[Lys(Cbz)-Glu(OBzl)] are nearly the same as those for PBLG but larger than those for PCBL. We may conclude from this finding that the helix stability of poly[Lys(Cbz)-Glu(OBzl)] is nearly the same as that of PBLG but that the PCBL helix is less stable than both.

Figure 5 shows double-logarithmic plots of A_2 vs. $\bar{N}_w$ for poly[Lys(Cbz)-Glu(OBzl)], PBLG,[6,23] and PCBL,[8,21] all in DMF at 25 °C. Although the scatter of the data points

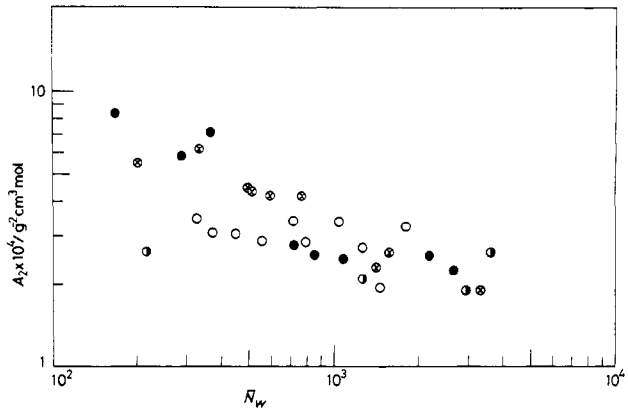

Figure 5. Second virial coefficients A_2 plotted against $\bar{N}_w$ for poly[Lys(Cbz)-Glu(OBzl)], PBLG, and PCBL in DMF at 25 °C. The symbols are the same as those used in Figure 4.

Table III
Viscosity and Sedimentation Data for Poly[Lys(Cbz)-Glu(OBzl)] in DMF at 25 °C

sample code	viscosity $[\eta]\times10^{-2}$/ cm^3 g^{-1}	k'	sedimentation $s_0\times10^{13}$/s	$k_s\times10^{-2}$/cm^{3}g^{-1}
LG-1[a]	6.45	0.42	4.58	2.32
LG-2	4.22	0.46	4.22	1.55
LG-3	3.51	0.48		
LG-4[b]	2.78	0.41	3.92	1.18
LG-5	2.05	0.33	3.77	0.83
LG-6	1.82	0.38	3.51	0.68
LG-7	1.33	0.38	3.38	0.46
LG-8	0.868	0.46		
LG-9	0.735	0.35		
LG-10	0.569	0.39	2.82	0.30

[a] Designated CF-H-2 in ref 14. [b] Designated CF-F-2 in ref 14.

prevents a definite conclusion, there is no appreciable difference among these polypeptides and the general trend is that A_2 is lower for higher $\bar{N}_w$.

Viscosity Data. The viscosity data for poly[Lys(Cbz)-Glu(OBzl)] in DMF at 25 °C are given in Table III. The values of the Huggins constant k' scatter in the range between 0.33 and 0.48 and indicate that poly[Lys(Cbz)-Glu(OBzl)] molecules are molecularly dispersed under this solvent condition. The molecular weight dependence of intrinsic viscosity is represented approximately by the Mark–Houwink–Sakurada equation

$$[\eta] = 1.60\times10^{-5}\bar{M}_w^{1.34} \qquad ([\eta] \text{ expressed in cm}^3\text{ g}^{-1})$$

The exponent 1.34 lies between those for PBLG (1.45)[23] and PCBL[8] (1.27). All the exponent values are smaller than 1.7 expected for sufficiently long straight rods. As shown above from the light scattering data, this implies that the helices of these polypeptides exhibit flexibility at higher molecular weight. Viscosity data for PBLG in DMF at 25 °C are given in Table I; those for samples A-IV through E-1 are reproduced from ref 23.

Sedimentation Velocity Data. The sedimentation coefficients s of seven poly[Lys(Cbz)-Glu(OBzl)] fractions in DMF at 25 °C were determined as a function of polymer concentration. The data were analyzed by $1/s = (1/s_0)(1 + k_s c)$ to obtain the limiting sedimentation coefficient s_0 and k_s. The data for s_0 of PBLG in DMF which will be used in the subsequent analysis have been taken from our previous study.[24] It was found, however, that the reported $\bar{M}_w$ were not correct.[25] We therefore calculated the viscosity-average molecular weights ($\bar{M}_v$) from the reported $[\eta]$ in DMF and in dichloroacetic acid, using the $[\eta]$–$\bar{M}_w$

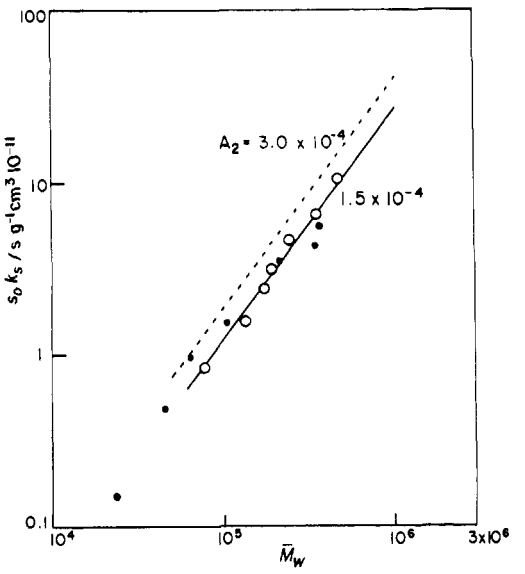

Figure 6. Test of eq 1 with the data for poly[Lys(Cbz)-Glu(OBzl)] (the unfilled circles) and PBLG (the filled circles). The solid and dashed lines indicate the values calculated for $A_2 = 1.5 \times 10^{-4}$ and 3×10^{-4} mol cm^{-3} g^{-2}, respectively; the slopes of these straight lines are $^4/_3$.

relationships given in Table I as the calibration standard.

Peterson[26] calculated the sedimentation velocity of a straight cylinder of length L and diameter d at finite concentration. His result can be combined with Zimm's equation[27] for A_2 to yield[24]

$$s_0 k_s = (1 - \bar{v}\rho_0)(3A_2/2\pi N_A)^{2/3} M^{4/3}/3\eta_0 \qquad (1)$$

where $\bar{v}$ is the specific volume of the cylinder, ρ_0 is the solvent density, η_0 is the solvent viscosity, M is the molecular weight of the cylinder, and N_A is Avogadro's number. Equation 1 predicts that $s_0 k_s$ should increase linearly with $M^{4/3}$. In Figure 6, this prediction is qualitatively satisfied with the data for poly[Lys(Cbz)-Glu(OBzl)] in DMF. However, quantitative agreement between theory and experiment cannot be achieved unless A_2 is taken to be 1.5×10^{-4} g^2 cm^{-3} mol^{-1}, which is about half the average A_2 determined from the light scattering measurements.

Discussion

Hydrodynamic Theories for Cylindrical Molecules. As shown above from the light scattering data, both poly[Lys(Cbz)-Glu(OBzl)] and PBLG form an intact α helix when $\bar{N}_w$ is lower than 1000. We examine whether or not the data for $[\eta]$ and s_0 of these polypeptides in DMF are consistent with this finding, using the hydrodynamic theories of cylindrical models.[12,13] Those for ellipsoidal models are not used because they are less realistic than the cylindrical models for α-helical polypeptides in solution. Norisuye et al.[12] derived on the basis of the Yamakawa–Fujii theory[28] an expression for s_0 for a "sausage model", which is a straight cylinder of diameter d with a hemisphere of the same diameter attached on each end. The length L of a sausage model is related to the degree of polymerization N of the corresponding cylindrical molecule by

$$Nh = L - d/3 \qquad (2)$$

where h is the length per monomeric residue of the cylindrical portion of the molecule; $L - d/3$ is the length of the equivalent cylindrical molecule with a uniform diameter d and the same volume. The expression for s_0 of Norisuye et al.[12] can be put in the form

$$s_0/M_0(1 - \bar{v}\rho_0) = (1/3\pi\eta_0 N_A h)(1 - d/3L)F_s(L/d,1) \qquad (3)$$

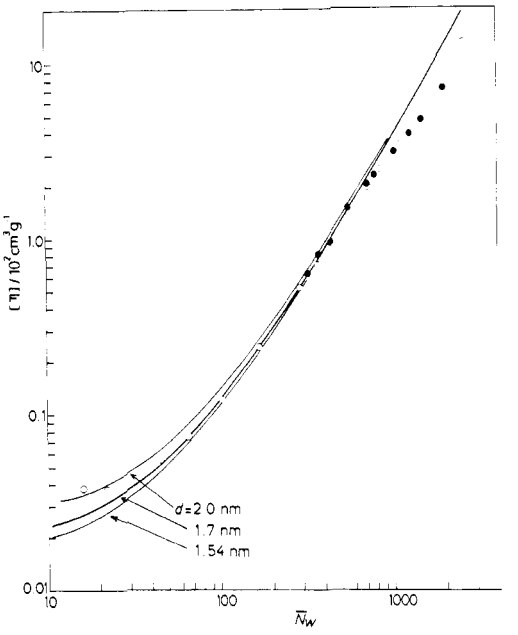

Figure 7. Comparison of the measured $[\eta]$ values for poly[Lys(Cbz)-Glu(OBzl)] (the filled circles) and PBLG (the unfilled circles) in DMF at 25 °C with the theoretical values calculated from eq 4 with $h = 0.15$ nm and the indicated values of d.

where M_0 is the molar mass per monomeric residue and $\bar{v}$ is the partial specific volume of the solute. $F_s(L/d,1) \equiv 3\pi\eta_0 L/\Xi_0$ is a function of L/d defined by eq 17 of ref 12.

Quite recently, Yoshizaki and Yamakawa[13] have extended the theory of Yamakawa and Fujii for cylindrical molecules[28,29] to cylindrical molecules with a hemispheroid attached on each end of the molecules (spheroid cylinders). The sausage model of Norisuye et al. is a special case of spheroid cylinders for which the hemispheroids are spherical. Yoshizaki and Yamakawa have obtained an expression for $[\eta]$ for the sausage model valid for any value of L/d; it gives the Einstein value for spheres at $L/d = 1$ and conforms to the correct asymptotic expression at large L/d.[29] The expression of Yoshizaki and Yamakawa can be rewritten

$$[\eta] = \frac{2\pi N_A N^2 h^3}{45M_0(1 - d/3L)F_\eta(L/d,1)} \qquad (4)$$

where $F_\eta(L/d,1)$ is a complicated function of L/d given in their paper.

Yoshizaki and Yamakawa have also derived expressions for the rotational diffusion coefficients of spheroid cylinders. From their result, we can obtain the expression for the dielectric relaxation time τ_1 of the sausage model with a permanent dipole along the cylinder axis. It reads

$$\tau_1 T/\eta_0 = \pi h^3 N^3 F_r(L/d,1)/6k(1 - d/3L)^3 \qquad (5)$$

where $F_r(L/d,1)$ is a function of L/d given in ref 13 and k is the Boltzmann constant.

Analysis of Experimental Data. Figure 7 shows the values of $[\eta]$ (corrected for the factor $219/M_0$) plotted against $\bar{N}_w$, where the circles denote the experimental data for poly[Lys(Cbz)-Glu(OBzl)] and PBLG in DMF at 25 °C and the curves represent the theorectical values calculated from eq 4 with $h = 0.15$ nm and the indicated values of d; M_0 for PBLG is 219. Poly[Lys(Cbz)-Glu(OBzl)] and PBLG exhibit essentially the same $[\eta]$–$\bar{N}_w$ relationships over the range of $\bar{N}_w$ examined. The data points for both poly[Lys(Cbz)-Glu(OBzl)] and PBLG follow closely the curve with $d = 1.7$ nm in the range of $\bar{N}_w$ lower than 800, where the molecular shape is found to

Table IV
Molecular Dimensions of α-Helical Polypeptides

method	PBLG		poly[Lys(Cbz)-Glu(OBzl)]		PCBL	
	h/nm	*d*/nm	*h*/nm	*d*/nm	*h*/nm	*d*/nm
viscosity[a]	0.15 ± 0.006	1.7 ∓ 0.2				
sedimentation[a]	0.16 ± 0.02	2.2 ∓ 0.7				
dielectric dispersion	0.15 ± 0.015	2.1 ∓ 0.5				
partial specific volume		1.54		1.64		1.72
X-ray[28]	0.153	1.36	0.154[b]	1.65[b]	0.155	1.90

[a] For poly[Lys(Cbz)-Glu(OBzl)] and PBLG. [b] Calculated from the data for PBLG and PCBL.

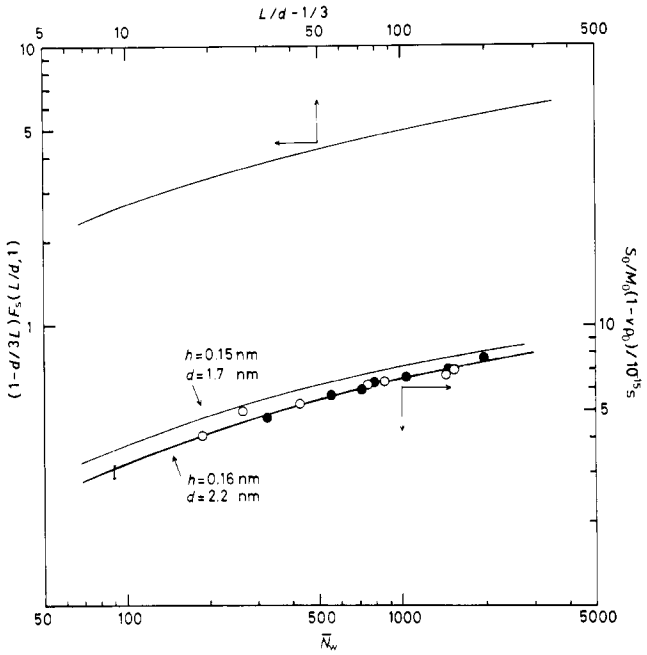

Figure 8. Double-logarithmic plots of $s_0/M_0(1 - \bar{v}\rho_0)$ vs. $\bar{N}_w$ for poly[Lys(Cbz)-Glu(OBzl)] (the filled circles) and PBLG (the unfilled circles) in DMF at 25 °C; the two curves represent the theoretical values calculated from eq 3 with the indicated parameter values. The theoretical curve for $(1 - d/3L)F_s(L/d,1)$ vs. $L/d - 1/3$ is shown on the upper part of this figure.

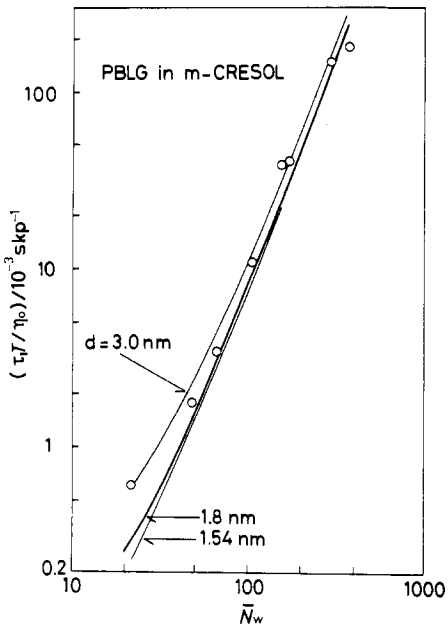

Figure 9. Comparison between the experimental τ_1 values for PBLG in *m*-cresol and Yoshizaki–Yamakawa's theoretical values calculated for $h = 0.15$ nm and the indicated d values.

be that of a straight rod from the light scattering data. The data points tend to deviate progressively downward from the theoretical curve as $\bar{N}_w$ increases above 800. The two points for the lowest molecular weight PBLG samples appear somewhat above the theoretical curve. It might be possible to explain this upswing in terms of the oblate spheroid cylinder model of Yoshizaki and Yamakawa.[13] However, a real PBLG molecule in DMF may not be represented so accurately by the theoretical model as the theory requires. This is because PBLG molecules of such low molecular weights ($\bar{N}_w$ = 15.8 for A-1 and 21.8 for A-2) are not perfectly helical in DMF at room temperature but contain several random coil residues on the chain ends,[30] which provide extra friction to the molecular motion.

The diameter of 1.54 nm corresponds to the rigid sausage model with a specific volume equal to the partial specific volume of PBLG. This diameter is somewhat too small to reproduce the viscosity data.

Alternatively, the values of h and d may be determined separately by comparing the plot of $\bar{N}_w^2/[\eta]$ vs. $\bar{N}_w$ and the curve of $(1 - d/3L)^3F_\eta(L/d,1)$ vs. $L/d - 1/3$ on a double-logarithmic graph. Using the data for $\bar{N}_w$ lower than 1000, we found that the combination of $h = 0.15 \pm 0.006$ nm and $d = 1.7 \mp 0.2$ nm yielded the best agreement between theory and experiment.

Figure 8 shows double-logarithmic plots of $s_0/M_0(1 - \bar{v}\rho_0)$ vs. $\bar{N}_w$ for poly[Lys(Cbz)-Glu(OBzl)] and PBLG in DMF at 25 °C. The data for both polypeptides, when corrected for the factor $M_0(1 - \bar{v}\rho_0)$, scatter around a smooth curve. On the upper part of the figure is shown the theoretical curve for $(1 - d/3L)F_s(L/d,1)$ vs. $L/d - 1/3$ calculated from eq 3. Comparison of the theoretical curve with the experimental data gives $h = 0.16 \pm 0.02$ nm and $d = 2.2 \mp 0.7$ nm. The curve with $h = 0.15$ nm and $d = 1.7$ nm appears slightly above the data points.

The data obtained by Matsumoto et al.[15] for the dielectric relaxation time of PBLG in *m*-cresol are reproduced in Figure 9. Using a curve-fitting procedure similar to that employed above for s_0, we obtained on the basis of eq 5 the result that $h = 0.15 \pm 0.015$ nm and $d = 2.1 \mp 0.5$ nm. Except for the case of intrinsic viscosity, no greater accuracy can be claimed for the derived parameters, especially for d, because the experimental data cover only a limited range of $\bar{N}_w$ and the theoretical curves are more or less featureless.

Table IV summarizes the values of d and h obtained; it also includes the values of d and h estimated from small-angle X-ray scattering measurements[31] and from the partial specific volume of each polypeptide with the assumption of $h = 0.15$ nm. The X-ray values were computed from $d/2 = 2^{1/2}\langle s_q^2\rangle^{1/2}$, where $\langle s_q^2\rangle$ is the mean-square radius of the cross section. All of the hydrodynamic data give h values close to 0.15 nm, indicating that the conformation of poly[Lys(Cbz)-Glu(OBzl)] and PBLG is α-helical. The value of 1.7 nm for d derived from the viscosity data is in substantial agreement with those obtained from the partial specific volume data and those from

the X-ray data. The *d* values from the sedimentation and dielectric dispersion data are somewhat larger than 1.7 nm, although the uncertainties of the derived values preclude a definite conclusion.

Acknowledgment. We thank Professor H. Yamakawa for making available his paper prior to publication. Thanks are also due Professor H. Fujita for helpul discussion.

References and Notes

(1) Tokyo Institute of Polytechnics, 1583 Atsugi-shi, Kanagawa 243-02, Japan.
(2) Osaka Electro-Communication University, Neyagawa, Osaka 572, Japan.
(3) Doty, P.; Bradbury, J. H.; Holtzer, A. M. *J. Am. Chem. Soc.* **1956**, *78*, 947.
(4) Benoit, H.; Freund, L.; Spach, G. In "Poly-α-Amino Acids"; Fasman, G. D., Ed.; Marcel Dekker: New York, 1967; Chapter 4.
(5) Miller, W. G.; Flory, P. J. *J. Mol. Biol.* **1966**, *15*, 284.
(6) Norisuye, T.; Teramoto, A.; Fujita, H. *Polym. J.* **1973**, *4*, 323.
(7) Teramoto, A.; Fujita, H. *Adv. Polym. Sci.* **1975**, *18*, 65.
(8) Matsuoka, M.; Norisuye, T.; Teramoto, A.; Fujita, H. *Biopolymers* **1973**, *12*, 1515.
(9) Nishioka, N.; Maekawa, A.; Teramoto, A. *Biopolymers* **1978**, *17*, 665.
(10) Teramoto, A.; Fujita, H. *J. Macromol. Sci., Rev. Macromol. Chem.* **1976**, *C15*, 165.
(11) Omura, I.; Lee, D. C.; Itou, S.; Teramoto, A.; Fujita, H. *Polymer* **1977**, *17*, 847.
(12) Norisuye, T.; Motowoka, M.; Fujita, H. *Macromolecules* **1979**, *12*, 320.
(13) Yoshizaki, T.; Yamakawa, H. *J. Chem. Phys.* **1980**, *72*, 57.
(14) Itou, S.; Lee, D. C.; Teramoto, A. *Macromolecules* **1977**, *10*, 1061.
(15) Matsumoto, T.; Nishioka, N.; Teramoto, A.; Fujita, H. *Macromolecules* **1974**, *7*, 824.
(16) See, for example: Murakami, H.; Norisuye, T.; Fujita, H. *Macromolecules* **1980**, *13*, 345.
(17) Deželič, Gj.; Vavra, J. *Croat. Chim. Acta* **1966**, *38*, 35.
(18) Berry, G. C. *J. Chem. Phys.* **1966**, *44*, 4550.
(19) Norisuye, T.; Matsuoka, M.; Teramoto, A.; Fujita, H. *Polym. J.* **1970**, *1*, 691.
(20) Einaga, Y.; Miyaki, Y.; Fujita, H. *J. Soc. Rheol. Jpn.* **1977**, *5*, 188. *J. Polym. Sci., Polym. Phys. Ed.* **1979**, *17*, 2103.
(21) Applequist, J.; Doty, P. In "Polyamino Acids, Polypeptides, and Proteins"; Stahman, M. A., Ed.; University of Wisconsin Press: Madison, Wisc., 1962; p 161.
(22) Moha, P.; Weill, G.; Benoit, H. *J. Chim. Phys.* **1964**, *61*, 1240.
(23) Norisuye, T. Ph.D. Thesis, Osaka University, 1973.
(24) Fujita, H.; Teramoto, A.; Yamashita, T.; Okita, K.; Ikeda, S. *Biopolymers* **1966**, *4*, 781.
(25) The values of M_w used in ref 24 had been determined from light scattering by assuming 48.5×10^{-6} cm^{-1} for Rayleigh's ratio R_{90} of 25 °C benzene at 436 nm and using a Zimm plot, i.e., Kc/R_θ vs. c (*Biopolymers* **1966**, *4*, 769). However, it was found later (ref 6 and 23) that they were 5–10% higher than those determined by sedimentation equilibrium and that consistent values of M_w could be obtained when 46.5×10^{-6} cm^{-1} was assumed for R_{90} and a $(Kc/R_\theta)^{1/2}$ vs. c plot was adopted. The values of M_w given in Table I of this paper are those obtained by either light scattering with the latter procedure or sedimentation equilibrium.
(26) Peterson, J. M. *J. Chem. Phys.* **1964**, *40*, 2680.
(27) Zimm, B. H. *J. Chem. Phys.* **1946**, *14*, 164.
(28) Yamakawa, H.; Fujii, M. *Macromolecules* **1973**, *6*, 407.
(29) Yamakawa, H.; Fujii, M. *Macromolecules* **1974**, *7*, 128.
(30) Matsumoto, T.; Teramoto, A. *Biopolymers* **1974**, *13*, 1347.
(31) Saludjian, P.; Luzzati, V. In "Poly-α-Amino Acids"; Fasman, G. D., Ed.; Marcel Dekker: New York, 1967; Chapter 3.

Rigid-Rod Polymers. 1. Synthesis and Thermal Properties of Para-Aromatic Polymers with 2,6-Benzobisoxazole Units in the Main Chain[1]

James F. Wolfe*

SRI International, Menlo Park, California 94025

F. E. Arnold

Materials Laboratory, Air Force Wright Aeronautical Laboratories, Air Force Systems Command, Wright-Patterson Air Force Base, Ohio 45433. *Received September 9, 1980*

ABSTRACT: The solution polycondensation of 4,6-diamino-1,3-benzenediol dihydrochloride with various para-aromatic dicarboxylic acids in poly(phosphoric acid) (PPA) or in PPA/sulfolane mixtures afforded soluble, thermally stable, rigid-rod polymers with 2,6-benzo[1,2-*d*:5,4-*d*']bisoxazole units in the main chain. Three *p*-terphenylene dicarboxylic acids with varied phenyl substitution on the middle phenylene ring were prepared. The polymers had intrinsic viscosities in methanesulfonic acid at 30 °C in the range 2.5–9.3 dL/g. The polymers showed excellent thermal stability, as determined by thermogravimetric analysis (TGA) in nitrogen and by thermogravimetric–mass spectral analysis (TGMS) in vacuo, and excellent thermooxidative stability, as determined by TGA and isothermal aging at 316 and 371 °C in air. The rigid-rod polymers with phenyl substituents showed limited solubility in PPA/sulfolane and *m*-cresol/strong acid mixtures; these mixtures were nonsolvents for similar polymers without phenyl substituents.

A series of 12 papers appearing in this issue reports the results of a research program[2] sponsored by the U.S. Air Force and directed toward the development of new structural materials having low density, high strength, high modulus, and long-term retention of these properties at elevated temperatures. Research in the past 2 decades has led to numerous aromatic heterocyclic polymer systems having excellent thermal and thermooxidative stability. In general, however, suitable fabrication techniques were lacking to obtain the high degree of molecular order in a bulk form required for extremely high mechanical properties.

It is well-established from both the theoretical considerations of Flory[3] and the extensive research conducted on extended-chain polyamides[4] that liquid crystalline solution behavior results from a high degree of molecular shape anisotropy, which is dependent on molecular structure and molecular weight, if another important

0024-9297/81/2214-0909$01.25/0